Inorganic Chemistry
Article

Inorg. Chem. **2010**, *49*, 583–594 **583**
DOI: 10.1021/ic901681e

Cyanide Lability and Linkage Isomerism of Hexacyanochromate(III) Induced by the Co(II) Ion

Carolina Avendano,[†] Ferdi Karadas,[†] Matthew Hilfiger,[†] Michael Shatruk,[‡] and Kim R. Dunbar*[,†]

[†]*Department of Chemistry, Texas A&M University, College Station, Texas 77842-3012, and* [‡]*Department of Chemistry & Biochemistry, Florida State University, Tallahassee, Florida 32306*

Received September 11, 2009

Reactions between the $[M^{III}(CN)_6]^{3-}$ (M=Fe and Co) anions and the mononuclear complex $[Co^{II}(dppe)_2(H_2O)][BF_4]_2$ result in the formation of two isostructural trinuclear clusters $\{[Co^{II}(dppe)_2]_2[M^{III}(CN)_6]\}(BF_4)$. Surprisingly, reactions of $[Co(dppe)_2(H_2O)](BF_4)_2$ and $[Co(triphos)(CH_3CN)_2](BF_4)_2$ with $[Cr(CN)_6]^{3-}$ yield the mononuclear complexes $[Co(dppe)_2(CN)](BF_4)$ and $[Co(triphos)(CN)_2]$, respectively. In the former case, an unusual pentanuclear intermediate complex $\{[Co^{II}{}_3(dppe)_4(MeCN)][Cr^{III}(CN)_6]_2\}$ was isolated. The reaction was probed by solution IR spectroscopy, which revealed a gradual conversion of the $\nu(C{\equiv}N)$ stretches of the starting materials to those of the CN-bridged intermediate and eventually to the single $\nu(C{\equiv}N)$ stretch of the final mononuclear product. The loss of carbon-bound CN^- ligands from $[Cr(CN)_6]^{3-}$ occurs on a sufficiently slow time-scale for observation of varying degrees of cyanide linkage isomerism in the trigonal bipyramidal complex $\{[Co(tmphen)_2]_3[Cr(CN)_6]_2\}$; the study was aided by the use of different Co(II) starting materials. Results obtained by a combination of X-ray crystallography, infrared spectroscopy, and magnetometry provide unequivocal evidence that the presence of certain Lewis acids (e.g., Co(II) in this work and Fe(II) ions and BPh_3 in previously reported studies) promote the process of cyanide linkage isomerism, which, in the case of Co(II) species, leads to facile labilization of cyanide ligands from the $[Cr(CN)_6]^{3-}$ anion.

Introduction

Transition metal cyanide chemistry is in a renaissance period that began over a decade ago and is now one of the central themes of molecular magnetism research. The increased activity is due, in large measure, to the discovery that certain analogues of the Prussian blue (PB) family exhibit spontaneous magnetization at temperatures as high as 376 K.[1−3] These findings helped to fuel interest in the topic of paramagnetic cyanide complexes, particularly mixed metal/transition metal clusters.[4−6] The preparation of finite complexes rather than face-centered cubic PB phases relies on the use of capping ligands, typically multidentate organic molecules that block a number of coordination sites on metal ions and prevent the growth of extended structures. Many multinuclear cyanide-bridged complexes with novel magnetic properties have been prepared by such an approach.[7]

In our quest for unusual cyanide compounds with various coligands, we turned to the tripodal phosphine ligand 1,1,1-tris(diphenylphosphinomethyl)ethane (triphos) for the preparation of molecular cubes $\{[MCl]_4[Re(triphos)(CN)_3]_4\}$[8−10] and squares $\{[M^{II}Cl_2]_2[Co^{II}(triphos)(CN)_2]_2\}$[11,12] (M = Mn, Fe, Co, Ni, Zn; Scheme 1). The formation of these species is dictated by the geometry of mononuclear building blocks, $[Re(triphos)(CN)_3]$[13] and $[Co(triphos)(CN)_2]$,[14] with three and two orthogonal CN^- ligands respectively that serve as bridges in the resulting multinuclear complexes.

*To whom correspondence should be addressed. E-mail: dunbar@mail.chem.tamu.edu.

(1) Mallah, T.; Thiebaut, S.; Verdaguer, M.; Veillet, P. *Science* **1993**, *262*, 1554–1557.
(2) Entley, W. R.; Girolami, G. S. *Science* **1995**, *268*, 397–400.
(3) Holmes, S. M.; Girolami, G. S. *J. Am. Chem. Soc.* **1999**, *121*, 5593–5594.
(4) Rebilly, J. N.; Mallah, T. *Struct. Bonding* **2006**, *122*, 103–131.
(5) Sieklucka, B.; Podgajny, R.; Przychodzen, P.; Korzeniak, T. *Coord. Chem. Rev.* **2005**, *249*, 2203–2221.
(6) Przychodzen, P.; Korzeniak, T.; Podgajny, R.; Sieklucka, B. *Coord. Chem. Rev.* **2006**, *250*, 2234–2260.
(7) Shatruk, M.; Avendano, C.; Dunbar, K. R. *Prog. Inorg. Chem.* **2009**, *56*, 155–334.
(8) Schelter, E. J.; Karadas, F.; Avendano, C.; Prosvirin, A. V.; Wernsdorfer, W.; Dunbar, K. R. *J. Am. Chem. Soc.* **2007**, *129*, 8139–8149.
(9) Schelter, E. J.; Prosvirin, A. V.; Dunbar, K. R. *J. Am. Chem. Soc.* **2004**, *126*, 15004–15005.
(10) Schelter, E. J.; Prosvirin, A. V.; Reiff, W. M.; Dunbar, K. R. *Angew. Chem., Int. Ed.* **2004**, *43*, 4912–4915.
(11) Karadas, F.; Schelter, E. J.; Prosvirin, A. V.; Bacsa, J.; Dunbar, K. R. *Chem. Commun.* **2005**, 1414–1416.
(12) Karadas, F.; Schelter, E. J.; Shatruk, M.; Prosvirin, A. V.; Bacsa, J.; Smirnov, D.; Ozarowski, A.; Krzystek, J.; Telser, J.; Dunbar, K. R. *Inorg. Chem.* **2008**, *47*, 2074–2082.
(13) Schelter, E. J.; Bera, J. K.; Bacsa, J.; Galan-Mascaros, J. R.; Dunbar, K. R. *Inorg. Chem.* **2003**, *42*, 4256–4258.
(14) Rupp, R.; Huttner, G.; Kircher, P.; Soltek, R.; Buchner, M. *Eur. J. Inorg. Chem.* **2000**, 1745–1757.

Published on Web 12/10/2009

Scheme 1. Formation of (a) Molecular Squares $\{[M^{II}Cl_2]_2[Co^{II}(triphos)(CN)_2]_2\}$ (M^{II} = Mn, Fe, Co, Ni, and Zn) and (b) Trimers $\{[Co^{II}(dppe)_2]_2[M^{III}(CN)_6\}^+$ (M^{III} = Fe, Co)

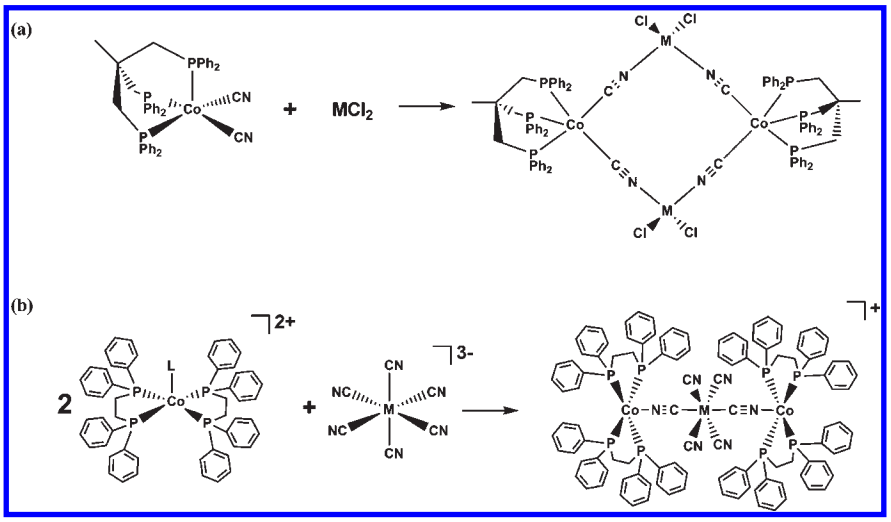

Of relevance to the present report, the tendency of the Co^{II} ion to form pentacoordinate complexes with phosphine ligands is well-known.[15,16] Our successful use of $[Co(triphos)(CN)_2]$ for the preparation of molecular squares prompted us to synthesize other cyanide-bridged complexes with phosphine groups. Trinuclear species are the simplest model systems for the study of magnetic properties as a function of the nature of metal ions and their coordination geometries; hence, we sought to identify starting materials that would lead to products with three metal ions. The bidentate ligand 1,2-bis(diphenylphosphino)ethane (dppe) affords the pentacoordinate building block $[Co(dppe)_2(H_2O)]^{2+}$ which, when combined with a hexacyanometallate anion in a 2:1 ratio, leads to the desired trinuclear complex (Scheme 1b). This approach, while convenient for Co^{II}, does not translate well to other first row transition metals, as they are not prone to forming pentacoordinate precursors with dppe or other phosphine ligands.[17]

We successfully used the outlined synthetic strategy to prepare cyanide-bridged molecular trimers with $[Fe^{III}(CN)_6]^{3-}$ and $[Co^{III}(CN)_6]^{3-}$ anions, but an unexpected result occurred with $[Cr^{III}(CN)_6]^{3-}$, namely, the formation of a trigonal-bipyramidal (TBP) cyanide-bridged cluster. In this molecule, three equatorial positions are occupied by Co^{II} ions and the two axial positions are filled by $[Cr^{III}(CN)_6]^{3-}$ ions. A study of the formation and structure of this complex revealed that the Co^{II} ions are bound to the C atoms of the bridging CN^- ligands as a consequence of cyanide linkage isomerism. Reversal of the orientation of the cyanide ligand has been observed for several other cyanide-bridged compounds containing Cr^{III}.[18,19] For example, many years ago, Brown and Shriver observed that a $Co^{II}{}_3[Cr^{III}(CN)_6]_2$ Prussian blue analogue undergoes a cyanide flip process when heated in an inert atmosphere to 100 °C,[20] and recently, Coronado and et al. discovered that the cyanide linkage isomerism of the Prussian blue analog $K_{0.4}Fe_4[Cr(CN)_6]_{2.8}\cdot 16H_2O$ can be reversed with the application of pressure.[19] Our group reported facile, albeit partial isomerization of the CN moiety for the $\{[Co^{II}(tmphen)_2][Cr^{III}(CN)_6]_2\}$ cluster with a TBP core.[21] A complete reversal of cyanide bridges was established for the related complex $\{[Fe^{II}(tmphen)_2][Cr^{III}(CN)_6]_2\}$,[22] as well as for the adduct of $[Cr^{III}(CN)_6]^{3-}$ with triphenylboron, $[Cr^{III}(NCBPh_3)_6]^{3-}$.[23]

Herein, we report a detailed investigation of cyanide linkage isomerism in the aforementioned $Co^{II}-Cr^{III}$ complexes with the aim of demonstrating the generality of this phenomenon for $[Cr^{III}(CN)_6]^{3-}$ in the presence of Lewis acids such as Fe^{II} and Co^{II} ions and BPh_3.

Experimental Section

Starting Materials. $K_3[Cr(CN)_6]$ (Aldrich), $K_3[Co(CN)_6]$ (Pfaltz and Bauer), $(TBA)_3[Fe(CN)_6]$ (Fluka; TBA = tetrabutylammonium), 18-crown-6 (Aldrich), 1,1,1-tris(diphenylphosphinomethyl)ethane (triphos; Aldrich), and $Co(BF_4)_2\cdot 6H_2O$ (Aldrich) were used as received. The ligand 1,2-bis(diphenylphosphino)ethane (dppe; Aldrich) was recrystallized from ethanol before use. $[Co(triphos)(CH_3CN)_2](BF_4)_2$ was prepared as previously reported.[14] Acetonitrile and methanol were dried over 3 Å molecular sieves and distilled prior to use. Unless stated otherwise, all compounds were prepared under anaerobic conditions.

$[Co^{II}(dppe)_2(H_2O)][BF_4]_2$ (1). A quantity of dppe (2.34 g, 5.6 mmol) was added to a solution of $Co(BF_4)_2\cdot 6H_2O$ (1.0 g, 2.8 mmol) in 70 mL of acetonitrile. The peach-colored mixture was stirred for 12 h, during which time a bright yellow precipitate was observed to form. The solid was collected by filtration in the air, washed with dichloromethane (3 × 10 mL) and diethyl ether (3 × 5 mL), and air-dried. Yield = 2.58 g (88%). Elem anal. calcd for $CoP_4F_8OC_{52}B_2H_{50}$: C, 59.63; H, 4.81; F, 14.51. Found: C, 60.89; H, 4.71; F, 14.27%.

(15) Jacob, V.; Huttner, G.; Kaifer, E.; Kircher, P.; Rutsch, P. *Eur. J. Inorg. Chem.* **2001**, 2783–2795.
(16) Jacob, V.; Mann, S.; Huttner, G.; Walter, O.; Zsolnai, L.; Kaifer, E.; Rutsch, P.; Kircher, P.; Bill, E. *Eur. J. Inorg. Chem.* **2001**, 2625–2640.
(17) DuBois, D. L.; Miedaner, A. *Inorg. Chem.* **1986**, *25*, 4642–4650.
(18) Harris, T. D.; Long, J. R. *Chem. Commun.* **2007**, 1360–1362.
(19) Coronado, E.; Gimenez-Lopez Mari, C.; Levchenko, G.; Romero Francisco, M.; Garcia-Baonza, V.; Milner, A.; Paz-Pasternak, M. *J. Am. Chem. Soc.* **2005**, *127*, 4580–4581.
(20) Brown, D. B.; Shriver, D. F. *Inorg. Chem.* **1969**, *8*, 37–42.
(21) Shatruk, M.; Chambers, K. E.; Prosvirin, A. V.; Dunbar, K. R. *Inorg. Chem.* **2007**, *46*, 5155–5165.
(22) Shatruk, M.; Dragulescu-Andrasi, A.; Chambers, K. E.; Stoian, S. A.; Bominaar, E. L.; Achim, C.; Dunbar, K. R. *J. Am. Chem. Soc.* **2007**, *129*, 6104–6116.
(23) Schelter, E. J.; Shatruk, M.; Heintz, R. A.; Galan-Mascaros, J. R.; Dunbar, K. R. *Chem. Commun.* **2005**, 1417–1419.

Table 1. Reaction Conditions Used along with Colors and IR Data for Different Batches of $\{[Co(tmphen)_2]_3[Cr(CN)_6]_2\}$

sample	solvent	Co(II) source	time	temperature	color	ν(C≡N),[a] cm^{-1}
8a[b]	MeCN	$CoCl_2$	24 h	25 °C	brown	2157(b), 2133(t), 2105(i)
8b	MeCN	$Co(BF_4)_2 \cdot 6H_2O$	24 h	25 °C	yellow/brown	2155, 2147(b), 2135, 2126 (t), 2103(i)
8c[c]	MeCN	$Co(BF_4)_2 \cdot 6H_2O$	5 min	25 °C	yellow	2155, 2147(b), 2123(t), 2103(i)
8d[c]	MeCN	$Co(BF_4)_2 \cdot 6H_2O$	1 min	0 °C	peach-yellow	2155, 2147(b), 2123(t)
8e	MeOH	$CoCl_2 \cdot 6H_2O$	24 h	25 °C	peach	2157(b), 2125(t)

[a] t = terminal, b = bridging normal, i = bridiging isomerized. [b] The sample was prepared under anaerobic conditions. [c] Reactions were performed with stirring.

$\{[Co^{II}(dppe)_2]_2[Co^{III}(CN)_6]\}(BF_4)$ (2). A solution of [(18-crown-6)K]$_3$[Co(CN)$_6$] was prepared by stirring 56.5 mg (0.170 mmol) of $K_3[Co(CN)_6]$ and 113 mg (0.430 mmol) of 18-crown-6 in 13 mL of methanol for 6 h. The resulting solution was filtered to remove excess $K_3[Co(CN)_6]$. A second solution was prepared by stirring 300 mg (0.28 mmol) of **1** in 7 mL of acetonitrile to give a dark orange solution. The [(18-crown-6)K]$_3$[Co(CN)$_6$] solution was slowly added to the dark orange solution, and the mixture was left to stand undisturbed for 3 days. The crop of orange-red crystals that formed was filtered in the air and washed with copious amounts of methanol. Yield = 225 mg (78%). Elemental analysis indicated the presence of interstitial water and methanol molecules. Elem anal. calcd for $Co_3P_8F_4O_5N_6C_{111}BH_{108}$ (**2**$\cdot CH_3OH \cdot 4H_2O$): C, 62.93; H, 5.14; N, 3.97; F, 3.58. Found: C, 63.69; H, 5.10; N, 4.29; F, 3.03%. IR(Nujol): ν(C≡N) 2126, 2148 cm^{-1}. ESI^+-MS (CH_3CN): m/z 1926 ($[M]^+$), 964 ($[M - H]^{2+}$). UV−vis(CH_3CN), λ_{max}, nm (ε, M^{-1} cm^{-1}): 255 (5.8×10^4), 315 (2.1×10^4), 383 (5951).

$\{[Co^{II}(dppe)_2]_2[Fe^{III}(CN)_6]\}(BF_4)$ (3). Compound **3** was prepared in a fashion analogous to that described above for compound **2**. The acetonitrile soluble salt $(TBA)_3[Fe(CN)_6]$ (62 mg per 10 mL of solvent) was used as the source of $[Fe(CN)_6]^{3-}$ anions. Yield = 205 mg (71%). Elem anal. calcd for $Co_2FeP_8F_4N_6C_{110}BH_{96}$: C, 65.28; H, 4.94; N, 4.11; F, 3.72. Found: C, 65.37; H, 4.80; N, 4.23; F, 3.52%. IR(Nujol): ν(C≡N) 2108, 2129 cm^{-1}. ESI^+-MS (CH_3CN): m/z 1923 ($[M]^+$), 962 ($[M - H]^{2+}$). UV−vis(CH_3CN), λ_{max}, nm (ε, M^{-1} cm^{-1}): 253 (5.4×10^4), 320 (2.7×10^4), 394 (6857).

$[Co^{II}(dppe)_2(CN)][BF_4]$ (4). This compound was synthesized using a different route than the previously reported procedure.[24] A solution of [(18-crown-6)K]$_3$[Cr(CN)$_6$] was prepared by stirring 81.3 mg (0.250 mmol) of $K_3[Cr(CN)_6]$ and 159 mg (0.6 mmol) of 18-crown-6 in 10 mL of methanol for 6 h. The resulting solution was filtered to remove excess $K_3[Cr(CN)_6]$. A second solution was prepared by stirring 321 mg (0.3 mmol) of **1** in 10 mL of acetonitrile to give a dark orange solution. The [(18-crown-6)K]$_3$[Cr(CN)$_6$] solution was slowly added to the dark orange solution, and the mixture was left to stand undisturbed. After 3 days, dark red-brown block crystals were present. The crystals were collected in the air and washed with acetonitrile/diethyl ether. Yield = 193 mg (42%). Elem anal. calcd for $CoP_4F_4NC_{53}BH_{48}$: C, 65.72; H, 4.99; F, 7.85; N, 1.45. Found: C, 65.20; H, 4.95; F, 7.78; N, 1.65%. IR(Nujol): ν(C≡N) 2096 cm^{-1}. ESI^+-MS (CH_3CN): m/z 882 ($[M]^+$). UV−vis (CH_3CN), λ_{max}, nm (ε, M^{-1} cm^{-1}): 502 (327).

$[Co^{III}(dppe)_2(CN)_2][BF_4]$ (5). A solution of [(18-crown-6)K]$_3$-[Cr(CN)$_6$] was prepared by stirring 81.3 mg (0.250 mmol) of $K_3[Cr(CN)_6]$ and 159 mg (0.6 mmol) of 18-crown-6 in 10 mL of methanol for 6 h. The resulting solution was filtered to remove excess $K_3[Cr(CN)_6]$. A second solution was prepared by stirring 321 mg (0.3 mmol) of **1** in 10 mL of acetonitrile to give a dark orange solution and the [(18-crown-6)K]$_3$[Cr(CN)$_6$] solution was slowly added to it. The resulting mixture was left to stand undisturbed for 3 days, after which time the solution was filtered in air. After one week, the filtrate had produced yellow block-shaped crystals which were collected by filtration and washed with copious amounts of methanol followed by 5 mL of diethyl ether. Yield = 98 mg (33%). Elem anal. calcd for $CoP_4F_4N_2C_{55}BH_{52}O$: C, 64.31; H, 5.10; F, 7.40; N, 2.72. Found: C, 64.64 ; H, 4.94 ; F, 7.38 ; N, 2.72%. IR(Nujol): ν(C≡N) 2114 cm^{-1}. ESI^+-MS (CH_3CN): m/z 908 ($[M]^+$). UV−vis(CH_3CN), λ_{max}, nm (ε, M^{-1} cm^{-1}): 299 (3.3×10^4), 353 (3.5×10^4).

$Co^{II}(triphos)(CN)_2$ (6). This compound was synthesized using a different route than the previously reported procedure.[15] A solution of [(18-crown-6)K]$_3$[Cr(CN)$_6$] was prepared by stirring 81.3 mg (0.250 mmol) of $K_3[Cr(CN)_6]$ and 159 mg (0.6 mmol) of 18-crown-6 in 10 mL of methanol for 6 h. The resulting solution was filtered to remove excess $K_3[Cr(CN)_6]$. A second solution was prepared by stirring 290 mg (0.3 mmol) of $[Co(triphos)(CH_3CN)_2](ClO_4)_2$ in 10 mL of acetonitrile to give a dark green solution. The [(18-crown-6)K]$_3$[Cr(CN)$_6$] solution was slowly added to the dark green solution to yield a dark orange solution. The mixture was left to stand undisturbed for 3 days, during which time dark-red block-shaped crystals formed. The crystals were collected in the air and washed with diethyl ether. Yield = 59 mg (27%). Elem anal. calcd for $CoP_3N_2C_{43}H_{39}$: C, 70.21; H, 5.34; N, 3.81. Found: C, 69.95; H, 5.55; N, 3.77%. IR(Nujol): ν(C≡N) 2096(s), 2101(w) cm^{-1}.

$\{[Co^{II}_3(dppe)_4(MeCN)][Cr^{III}(CN)_6]_2\}$ (7). A solution of [(18-crown-6)K]$_3$[Cr(CN)$_6$] was prepared by stirring 55.2 mg (0.170 mmol) of $K_3[Cr(CN)_6]$ and 113 mg (0.430 mmol) of 18-crown-6 in 7 mL of acetonitrile for 6 h and was filtered to remove excess $K_3[Cr(CN)_6]$. This solution was slowly added to a dark orange solution of 300 mg (0.28 mmol) of **1** in 3 mL of acetonitrile. Crystals were observed after 30 min. Surprisingly, the few orange crystals obtained were of sufficient quality for single-crystal X-ray analysis.

$\{[Co^{II}(tmphen)_2]_3[Cr^{III}(CN)_6]_2\}$ (8). Five different samples of this complex were prepared according to the general method reported earlier[21] by varying the solvent, temperature, and reaction time (Table 1). In all reactions, a 4 mM solution of Co(II) salt was treated with 2 equiv of tmphen, and the solution was stirred for ~30 min, after which time a 4 mM solution of [K(18-crown-6)]$_3$[Cr(CN)$_6$] was added. The product that formed was recovered by filtration, washed with the same solvent as used for the reaction, and dried in vacuo. No structural characterization of these samples was undertaken, but, as established in our previous reports,[21] they contain varying amounts of interstitial solvent, which exchanges for water with the exposure of solid samples to humid laboratory air.

Physical Measurements. Elemental analyses were performed by Atlantic Microlab, Inc. IR spectra were measured as Nujol mulls or solutions placed between KBr plates on a Nicolet 740 FT-IR spectrometer. Electrospray mass spectra were acquired on an MDS Sciex API QStar Pulsar mass spectrometer using an electrospray ionization source. All spectra were acquired in the positive ion mode in an acetonitrile solution at an approximately 50 μM analyte concentration. The spray voltage was ~4800 V, and the nozzle skimmer potential was adjusted to 10 V to minimize fragmentation. Solution UV−visible absorption spectra were obtained by using a Shimadzu UV-1601PC

(24) Rigo, P.; Bressan, M. *Inorg. Nucl. Chem. Lett.* **1973**, *9*, 527–532.

Table 2. Crystal Structural Data and Refinement Parameters for Compounds **2**−**5** and **7**

formula	$Co_3P_8F_4O_2N_6C_{112}BH_{104}$ (**2**·2MeOH)	$Co_2FeP_8F_4O_2N_6C_{112}BH_{104}$ (**3**·2MeOH)	$CoP_4F_4NC_{53}BH_{48}$ (**4**)
space group	$P2_1/n$	$P2_1/n$	$P2_1/c$
unit cell	a = 12.653(1) Å	a = 12.718(4) Å	a = 12.572(2) Å
	b = 21.718(2) Å	b = 21.726(7) Å	b = 25.590(3) Å
	c = 19.395(1) Å	c = 19.360(6) Å	c = 14.669(2) Å
	β = 92.207(1)°	β = 91.837(5) °	β = 106.029(2))°
unit cell volume, V	5325.7(6)Å^3	5347(3) Å^3	4536.0(10)Å^3
Z	2	2	1
density, ρ_{calcd}	1.335 g/cm^3	1.353 g/cm^3	1.418 g/cm^3
absorption coefficient, μ	0.644 mm^{-1}	0.627 mm^{-1}	0.575 mm^{-1}
cryst color and habit	orange-red needle	dark-green needle	red-brown block
cryst size	0.18 × 0.10 × 0.08 mm	0.16 × 0.11 × 0.07 mm	0.11 × 0.10 × 0.09 mm
temp	110 K	110 K	110 K
radiation, λ	Mo Kα, 0.71073 Å	Mo Kα, 0.71073 Å	Mo Kα, 0.71073 Å
min. and max. θ	1.86 to 25.00°	1.41 to 28.43°	1.59 to 28.30°
reflns collected	44963 [R_{int} = 0.0320]	32303 [R_{int} = 0.2242]	25866 [R_{int} = 0.0342]
independent reflns	9010	9158	10270
data/params/restraints	9010/724/237	9158/641 /746	10270/577/1
R [$F_o > 4\sigma(F_o)$]	R_1 = 0.086	R_1 = 0.092	R_1 = 0.060
	wR_2 = 0.203	wR_2 = 0.194	wR_2 = 0.146
Goodness-of-fit on F^2	1.280	1.084	1.087
max./min. residual densities, e·Å^{-3}	1.63, −0.78	1.23, −0.92	1.96, −0.51

formula	$CoP_4F_4N_3C_{56}BH_{43}$ (**5**)	$Co_3Cr_2P_8O_{4.5}N_{15.5}C_{127.5}H_{124.5}$ (**7**·4.5MeOH·2.5MeCN)
space group	$P\bar{1}$	$Aba2$
unit cell	a = 10.498(1) Å	a = 51.547(10) Å
	b = 13.092(2) Å	b = 26.188(5) Å
	c = 19.029(2) Å	c = 19.705(4) Å
	α = 97.372(2)°	
	β = 92.307(2)°	
	γ = 111.080(1)°	
unit cell volume, V	2409.9(5) Å^3	26600(9) Å^3
Z	2	8
density, ρ_{calcd}	1.416 g/cm^3	1.236 g/cm^3
abs. coeff., μ	0.547 mm^{-1}	0.676 mm^{-1}
cryst color and habit	yellow block	orange plate
cryst size	0.20 × 0.20 × 0.10 mm	0.15 × 0.11 × 0.07 mm
temperature	110 K	110 K
radiation, λ	Mo Kα, 0.71073 Å	Mo Kα, 0.71073 Å
min. and max. θ	1.69 to 28.44°	1.35 to 26.37°
reflns collected	25826[R_{int} = 0.0297]	101233 [R_{int} = 0.1948]
independent reflns	10940	23377
data/params/restraints	10940/626 /0	23377 /1397/4
R [$F_o > 4\sigma(F_o)$]	R_1 = 0.042	R_1 = 0.126
	wR_2 = 0.1116	wR_2 = 0.283
GoF on F^2	1.034	1.027
max./min residual densities, e·Å^{-3}	1.14, −0.68	1.91, −0.76

spectrophotometer in the 200−1000 nm range. Magnetic measurements were performed on crushed microcrystalline samples with the use of a Quantum Design MPMS-XL SQUID magnetometer. DC magnetic susceptibility measurements were performed in the range of 1.8−300 K in an applied field of 0.1 T. Magnetization data were collected in the 0−7 T range starting at zero field at 1.8 K. Data were corrected for the diamagnetic contributions calculated from the Pascal constants.[25] The molecular weight of each compound was adjusted according to the interstitial solvent content, as determined from thermal gravimetric analysis data.

X-Ray Crystallography. In a typical experiment, a crystal selected for study was suspended in polybutene oil (Aldrich) and mounted on a cryoloop which was placed in a N_2 cold stream. Single-crystal X-ray data were collected on a Bruker APEX or Bruker SMART 1000 diffractometer equipped with a CCD detector at 110 K. The data sets were recorded as three ω scans of 606 frames each, at a 0.3° step width, and integrated with the Bruker SAINT[26] software package. The absorption correction (SADABS[27]) was based on fitting a function to the empirical transmission surface as sampled by multiple equivalent measurements. Solution and refinement of the crystal structures was carried out using the SHELX[28] suite of programs and the graphical interface X-SEED.[29] Structure solution by direct methods resolved positions of all metal and P atoms as well as most of the C and N atoms. The remaining non-hydrogen atoms were located by alternating cycles of least-squares refinements and difference Fourier maps. Hydrogen atoms were placed at calculated positions. In the case of compounds with $[BF_4]^-$ counterions, these were disordered and were restrained to meaningful geometries. The final refinement was performed with anisotropic thermal parameters for all non-hydrogen atoms. A summary of pertinent information relating to unit cell parameters, data collection, and refinements is provided in Table 2. Selected metal−ligand bond distances are provided in Table 3

(25) Bain, G. A.; Berry, J. F. *J. Chem. Educ.* **2008**, *85*, 532–536.
(26) *SMART*; *SAINT*; Siemens Analytical X-ray Instruments Inc.: Madison, WI, 1996.
(27) Sheldrick, G. M. *SADABS*; University of Gottinggen: Gottingen, Germany, 1996.
(28) Sheldrick George, M. *Acta Crystallogr., Sect. A* **2008**, *64*, 112–122.
(29) Barbour, L. J. *J. Supramol. Chem.* **2003**, *1*, 189–191.

Table 3. Metal-Ligand Bond Distances (Å) and Bond Angles (deg) in the Crystal Structures of Compounds **2**–**5**[a]

{[Co(dppe)$_2$]$_2$[Co(CN)$_6$]}(BF$_4$) (**2**)				{[Co(dppe)$_2$]$_2$[Fe(CN)$_6$]}(BF$_4$) (**3**)			
Co(1)−N≡C	1.983(5)	Co(1)−N≡C	178.5(5)	Co(1)−N≡C	1.982(4)	Co(1)−N≡C	176.9(5)
Co(2)−C≡N$_{br}$	1.925(7)	Co(2)−C≡N$_{br}$	176.4(6)	Fe−C≡N$_{br}$	1.997(5)	Fe−C≡N$_{br}$	175.9(5)
Co(2)−C≡N$_{ter}$	2.08(1)	Co(2)−C≡N$_{ter}$	176.1(9)	Fe−C≡N$_{ter}$	2.102(7)	Fe−C≡N$_{ter}$	175.4(6)
(C≡N)$_{br}$	1.099(9)	P(1)−Co−P(2)	81.83(6)	(C≡N)$_{br}$	1.069(7)	P(1)−Co−P(2)	81.00(6)
(C≡N)$_{ter}$	1.08(1)	P(2)−Co−P(3)	97.72(6)	(C≡N)$_{ter}$	1.031(8)	P(2)−Co−P(3)	99.21(6)
Co(1)−P$_{avg}$	2.27(1)	P(3)−Co−P(4)	81.16(6)	Co(1)−P$_{avg}$	2.279(1)	P(3)−Co−P(4)	81.62(7)
		P(4)−Co−P(1)	99.03(6)			P(4)−Co−P(1)	97.95(6)
[Co(dppe)$_2$(CN)][BF$_4$] (**4**)				[Co(dppe)$_2$(CN)$_2$][BF$_4$] (**5**)			
Co−C≡N$_{ter}$	1.986(3)	Co−C≡N$_{ter}$	178.3(3)	Co−C≡N$_{ter}$	1.889(2)	Co−C≡N$_{ter}$	175.2(2)
Co(1)−P$_{avg}$	2.278(1)	P(1)−Co−P(2)	86.00(3)	Co(1)−P$_{avg}$	2.317(1)	P(1)−Co−P(2)	82.99(2)
		P(2)−Co−P(3)	106.35(3)			P(2)−Co−P(3)	97.01(2)
		P(3)−Co−P(4)	89.12(3)			P(3)−Co−P(4)	82.99(2)
		P(4)−Co−P(1)	167.95(3)			P(4)−Co−P(1)	97.01(2)

[a] ter = terminal, br = bridging.

Table 4. Metal-to-Ligand Bond Distances (Å) and Bond Angles (deg) in the Crystal Structures of Compound **7**

{[Co$_3$(dppe)$_4$(MeCN)][Cr(CN)$_6$]$_2$} (**7**)							
Cr(1)−(C≡N)$_{terminal}$	2.047(17)	Cr(1)−N(1)≡C(1)−Co(1)	174.8(12)	Co(2)−P(4)	2.310(5)	C(3)−Co(2)−C(6)	87.4(5)
Cr(1)−N(1)≡C(1)−Co(1)	2.042(15)	Cr(1)−N(3)≡C(3)−Co(2)	171.1(10)	Co(2)−P(6)	2.230(4)	C(3)−Co(2)−P(5)	90.4(4)
Cr(1)− N(3)≡C(3)−Co(2)	2.023(12)	Cr(1)−N(2)≡C(2)−Co(3)	175.3(10)	Co(2)−P(5)	2.228(4)	C(6)−Co(2)−P(5)	155.9(4)
Cr(1)− N(2)≡C(2)−Co(3)	2.021(16)			Co(2)−C(3)≡N−Cr(1)	1.830(14)	C(3)−Co(2)−P(6)	162.4(5)
Cr(2)− (C≡N)$_{terminal}$	2.032(16)	Cr(2)−N(4)≡C(4)−Co(1)	169.4(10)	Co(2)−C(6)≡N−Cr(2)	1.867(14)	C(6)−Co(2)−P(6)	92.3(4)
Cr(2)− N(4)≡C(4)−Co(1)	2.005(12)	Cr(2)−N(6)≡C(6)−Co(2)	175.0(10)			P(5)−Co(2)−P(6)	82.79(15)
Cr(2)− N(6)≡C(6)−Co(2)	2.036(13)	Cr(2)−N(5)≡C(5)−Co(3)	174.1(11)			C(3)−Co(2)−P(4)	95.8(4)
Cr(2)− N(5)≡C(5)−Co(3)	2.034(15)					C(6)−Co(2)−P(4)	98.2(4)
						P(5)−Co(2)−P(4)	105.85(17)
Co(1)−P(1)	2.242(4)	C(4)−Co(1)−C(1)	90.2(5)			P(6)−Co(2)−P(4)	101.61(16)
Co(1)−P(2)	2.230(4)	C(4)−Co(1)−P(2)	173.6(4)	Co(3)−P(8)	2.225(4)	C(5)−Co(3)−C(2)	88.7(6)
Co(1)−P(3)	2.269(4)	C(1)−Co(1)−P(2)	93.1(4)	Co(3)−P(7)	2.242(4)	C(5)−Co(3)−N(13)	96.4(5)
Co(1)−C(1)≡N(1)−Cr(1)	1.910(12)	C(4)−Co(1)−P(1)	88.7(4)	Co(3)−N(13)−CMe	2.035(11)	C(2)−Co(3)−N(13)	98.1(5)
Co(1)−C(4)≡N(4)−Cr(2)	1.865(16)	C(1)−Co(1)−P(1)	103.9(3)	Co(3)−C(2)≡N−Cr(1)	1.916(15)	C(5)−Co(3)−P(8)	89.6(4)
		P(2)−Co(1)−P(1)	85.21(15)	Co(3)−C(5)≡N−Cr(2)	1.868(14)	C(2)−Co(3)−P(8)	170.5(4)
		C(4)−Co(1)−P(3)	84.4(4)			N1(3)-Co(3)−P(8)	91.4(3)
		C(1)−Co(1)−P(3)	97.0(3)			C(5)−Co(3)−P(7)	171.0(4)
		P(2)−Co(1)−P(3)	100.60(16)			C(2)−Co(3)−P(7)	93.3(4)
		P(1)−Co(1)−P(3)	158.01(16)			N(13)−Co(3)−P(7)	92.1(4)
						P(8)−Co(3)−P(7)	87.08(16)

for compounds **2**–**5** and in Table 4 for compound **7**. Complete listings of atomic and thermal parameters, bond distances, and bond angles are available in the cif files (Supporting Information).

Results and Discussion

Syntheses and Single-Crystal X-ray Structures. The Co^{II} center in [Co^{II}(dppe)$_2$(X)]$^{2+}$, where X = MeCN or H$_2$O, is in a square-pyramidal geometry, which is typical for most phosphine complexes of Co^{II}, including those with chelating and monodentate phosphine ligands.[14,30−32] The presence of two dppe capping ligands and a single open site available for further chemistry renders this compound a convenient precursor for the assembly of linear trinuclear molecules.

An orange solution of [Co^{II}(dppe)$_2$(H$_2$O)][BF$_4$]$_2$ (**1**) in acetonitrile was reacted with solutions of [M^{III}(CN)$_6$]$^{3-}$ (M = Co and Fe) in methanol to form the isostructural linear cyanide-bridged trimers **2** and **3** (Figure 1). The compounds are stable in solution and in the solid state and are soluble in MeCN, CH$_2$Cl$_2$, and DMF. In both **2** and **3**, the ligand environment and geometries of each metal ion are the same as in the starting material, with the P atoms of dppe occupying the equatorial plane and the N-bound bridging cyanide from the hexacyanometallate fragment coordinating to the apical position of the square pyramid.

Surprisingly, the reaction of an acetonitrile solution of **1** and a methanol solution of [Cr^{III}(CN)$_6$]$^{3-}$ led to the formation of red crystals of the mononuclear complex [Co^{II}(dppe)$_2$(CN)][BF$_4$] (**4**). After removal of the crystals and exposure of the mother liquor to air for a week, yellow crystals of [Co^{III}(dppe)$_2$(CN)$_2$][BF$_4$] (**5**) were obtained.

In the structure of **4**, the geometry around the Co^{II} ion is substantially altered, as the dppe ligands have

(30) Mangani, S.; Orioli, P.; Ciampolini, M.; Nardi, N.; Zanobini, F. *Inorg. Chim. Acta* **1984**, *85*, 65–72.
(31) Stalick, J. K.; Corfields, P. W. R.; Meek, D. W. *Inorg. Chem.* **1973**, *12*, 1668–1675.
(32) Ciancanelli, R.; Noll, B. C.; DuBois, D. L.; DuBois, M. R. *J. Am. Chem. Soc.* **2002**, *124*, 2984–2992.

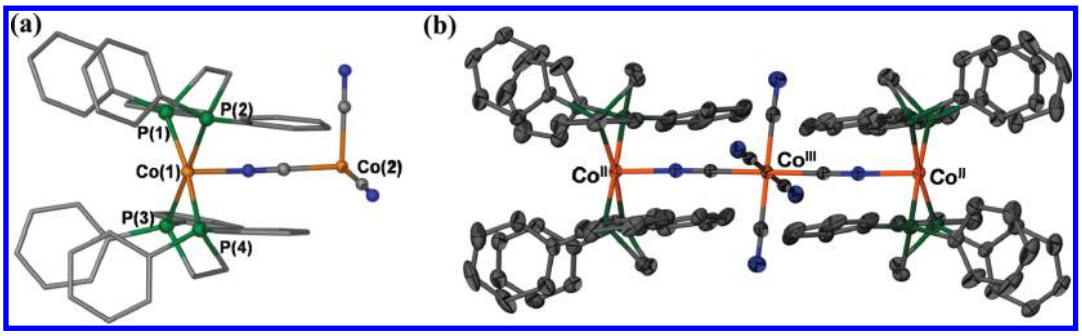

Figure 1. (a) Molecular structure of the asymmetric unit of $\{[Co^{II}(dppe)_2]_2[Co^{III}(CN)_6]\}^+$ and (b) the thermal ellipsoid plot of the trinuclear cation $\{[Co^{II}(dppe)_2]_2[Co^{III}(CN)_6]\}^+$ in **2**. Ellipsoids projected at the 50% probability level.

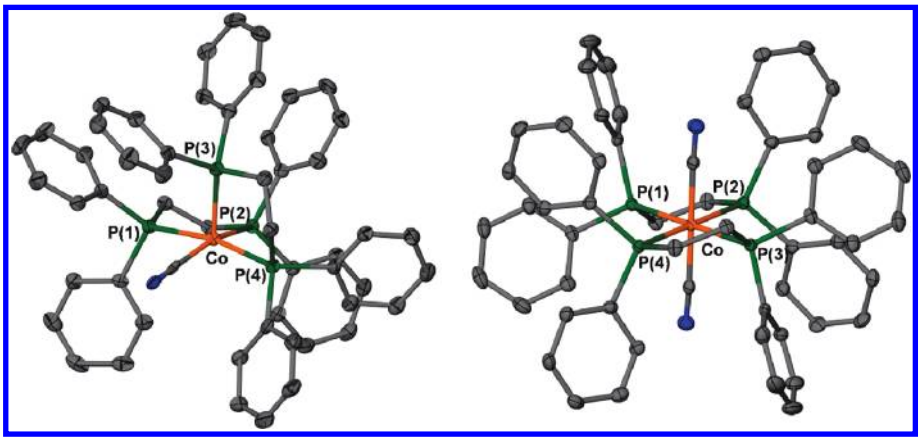

Figure 2. Thermal ellipsoid plots of the cation (a) $[Co(dppe)(CN)]^+$ in **4** and (b) $[Co(dppe)(CN)_2]^+$ in **5**. Ellipsoids projected at the 50% probability level.

rearranged around the cobalt ion and the CN^- ligand is positioned in the equatorial plane of the square pyramid (Figure 2a). The source of this cyanide is obviously the $[Cr^{III}(CN)_6]^{3-}$ ion as it is the only cyanide-containing starting material used in the reaction. Moreover, $[Cr^{III}(CN)_6]^{3-}$ has been shown to undergo cyanide linkage isomerism, leading to new cyano complexes that contain an N-bound Cr^{III} ion.[19,22,23] The observed products invoke two possible mechanisms, one in which a cyanide ligand of $[Cr^{III}(CN)_6]^{3-}$ is labilized, which frees it up to coordinate to the $[Co(dppe)_2(solv)]^{2+}$ complex, and another in which an intermediate bridging state is formed which assists in the cyanide flip and eventual formation of **4**. The latter mechanism is strongly supported by the present experimental evidence, as we were able to isolate an intermediate compound for the cyanide-bridged complex. The reaction of $[Co^{II}(dppe)_2(H_2O)]^{2+}$ and $[Cr^{III}(CN)_6]^{3-}$ in acetonitrile led to the isolation of crystals of the kinetic product $\{[Co^{II}_3(dppe)_4(MeCN)][Cr^{III}(CN)_6]_2\}$ (**7**). Compound **7** exhibits a TBP structure in which the $[Cr^{III}(CN)_6]^{3-}$ ions reside in the apical sites of the bipyramid and the equatorial sites are occupied by the Co^{II} ions (Figure 3a). Each Co center is coordinated to one chelating dppe ligand and two bridging cyanides from the apical hexacyanochromate fragments. The fifth site on the Co(2) and Co(3) ions is occupied by a P atom of a shared bridging dppe ligand, while the fifth site on Co(1) is occupied by an acetonitrile molecule (Figure 3b).

As the reaction progresses, it leads to the decomposition of the TBP cluster and subsequent formation of the final product **4**, with the result that all of the dppe ligands assume a typical chelating mode to a single Co^{II} ion (Scheme 2). It is proposed that compound **7** is an unstable intermediate that crystallizes during the course of the reaction. The isolation of this molecule provides crucial insight into the mechanism of linkage isomerism.

Further characterization of the $\{[Co^{II}_3(dppe)_4(MeCN)][Cr^{III}(CN)_6]_2\}$ species was hampered by an insufficient amount of material due to its facile conversion to compound **4**. Attempts to isolate pure samples of **7** by using other solvents were unsuccessful. In a similar manner, we found that, when an acetonitrile solution of $[Co(triphos)(CH_3CN)_2]^{2+}$ is treated with a methanol solution of $[Cr(CN)_6]^{3-}$ in a 2:1 ratio, the result is not the expected cyanide-bridged species but rather the previously reported mononuclear precursor Co(triphos)-$(CN)_2$.[14] Unfortunately, we were not able to isolate any intermediates in this reaction.

The isomerization and loss of cyanide ligands from $[Cr^{III}(CN)_6]^{3-}$ is not particularly surprising, as we had previously noted the cyanide flip issue in the reactions used to prepare the trigonal-bipyramidal complexes $\{[M(tmphen)_2]_3[Cr(CN)_6]_2\}$ (M = Fe, Co). Whereas the Fe-containing complex exhibited fast and essentially complete reversal of the bridging CN^- ligands,[22] the Co-containing TBP showed varying degrees of linkage isomerism depending on the experimental conditions.[21] To carry out a more detailed analysis of the isomerization process and to probe its ramifications on the properties of $\{[Co(tmphen)_2]_3[Cr(CN)_6]_2\}$ (**8**), we prepared several samples of the material by varying the solvent, time, and temperature of the reaction (Table 1).

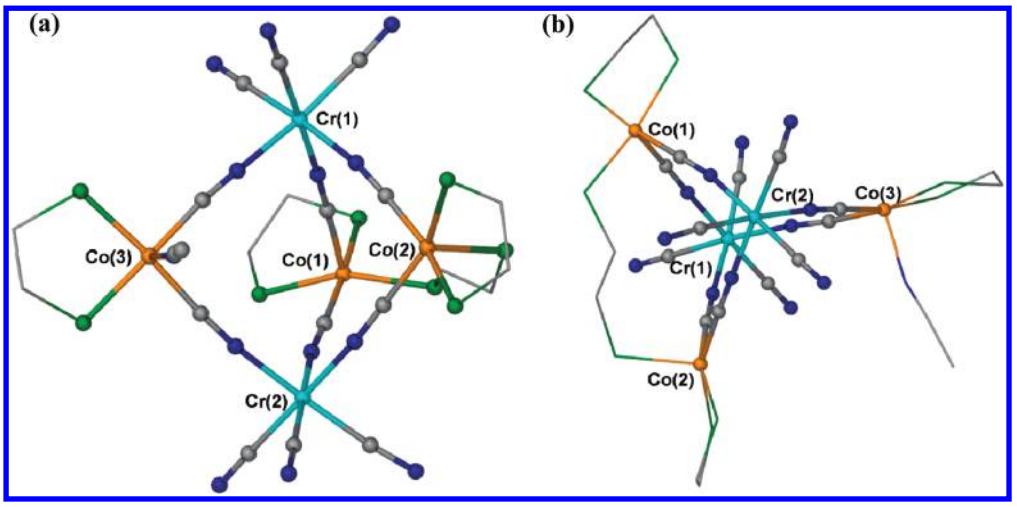

Figure 3. (a) Side view and (b) top view of the structure of $\{[Co^{II}_3(dppe)_4(MeCN)][Cr^{III}(CN)_6]_2\}$. (Phenyl rings omitted for the sake of clarity.)

Scheme 2. Conversion of Mononuclear Complex **1** to Mononuclear Complex **4** via the Formation of the Pentanuclear TBP Intermediate **7**

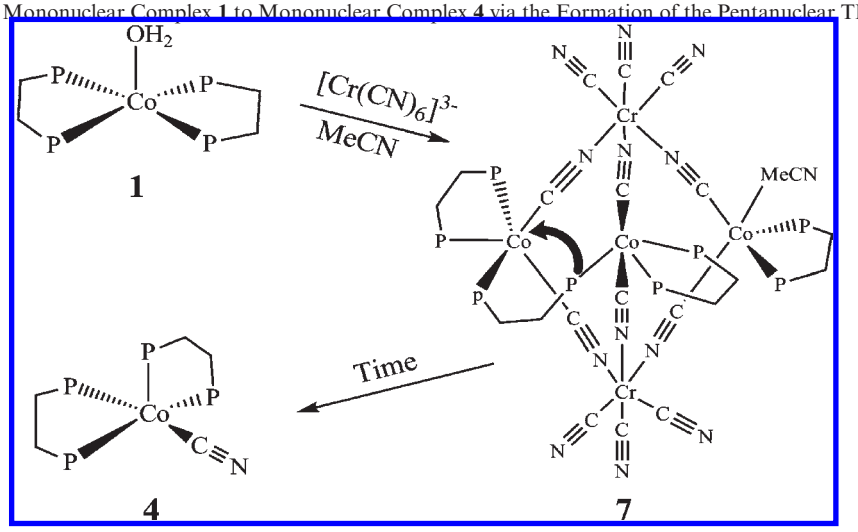

The first suspicion of cyanide linkage isomerism during the preparation of **8** came from the observation of the mixed colors of the product which first crystallized as a yellow solid but, after some time, reverted to an admixture of a yellow and brown (sample **8b** in Table 1). When the reaction was carried out with stirring for a short time (5 min) and immediately filtered, the product was recovered as a yellow solid (**8c**). Lowering the reaction temperature to 0 °C and shortening the reaction time to 1 min lead to the isolation of a peach-yellow product (**8d**). In order to slow down the reaction and favor the formation of the brown product observed in **8b**, we used anhydrous $CoCl_2$ as a starting material because the chloride ligands tend to be less labile than water. Indeed, this reaction (**8a**) resulted in the crystallization of a brown product. When the same reaction is performed in the more polar solvent methanol (**8e**), which enhances dissociation of the $CoCl_2$ starting material, rapid precipitation of a peach solid ensues. The color of the product did not change even after storage in the mother liquor for 24 h. These collective observations suggest the occurrence of cyanide linkage isomerism that can be controlled by reaction conditions. This hypothesis has been confirmed by a combination of IR spectroscopic and magnetic measurements (see below).

Table 5. ν(C≡N) Stretching Frequencies in the Complexes $\{[Co^{II}(dppe)_2]_2[M'^{III}(CN)_6]\}$ (M′ = Co, Fe), Corresponding PB Analogues, and Free Hexacyanometallate Anions

	ν(C≡N), cm^{-1}		
complex	bridging	terminal	$[M'(CN)_6]^{3-}$ anion[a]
(**2**) Co^{II}–Fe^{III}–Co^{II}	2129	2108	2101
(**3**) Co^{II}–Co^{III}–Co^{II}	2148	2126	2126

[a] As measured for $(TMA)_3[Fe(CN)_6]$ and $[(18\text{-crown-6})K]_3[Co(CN)_6]$ (TMA = tetramethylammonium).

Infrared Spectroscopy. Compounds **2** and **3** exhibit characteristic bands in the ν(C≡N) stretching region. A comparison of the observed IR data to the ν(C≡N) stretches reported for extended Prussian blue phases and the free hexacyanometallate anions aids in the assignment of the bands in the new compounds to bridging or terminal CN^- ligands. As the data in Table 5 indicate, the IR spectra of **2** and **3** exhibit lower-frequency stretches that are only slightly shifted as compared to the corresponding modes of the $[M^{III}(CN)_6]^{3-}$ ions (M = Co, Fe) and, therefore, are reasonably assigned to the terminal cyanides. Upon formation of the M^{III}–C≡N–Co^{II} bridge, the CN stretching frequency increases.[7]

Table 6. ν(C≡N) Stretching Frequencies for Complexes **4** and **5** and a Summary of the Solution IR Study of the Reaction of $[Co^{II}(dppe)_2(H_2O)]^{2+}$ with $[Cr^{III}(CN)_6]^{3-}$ in Acetonitrile

	ν(C≡N), cm^{-1}	
complex	bridging	terminal
(**4**) $[Co^{II}(dppe)_2(CN)][BF_4]$		2096
(**5**) $[Co^{III}(dppe)_2(CN)_2][BF_4]$		2114
$[Co(dppe)_2(H_2O)]^{2+} + [Cr(CN)_6]^{3-}$ in Acetonitrile		
$[Cr^{III}(CN)_6]^{3-}$		2115[a]
initial	2140	2113
30 min	2140, 2130	2113, 2090
1 h	2130	2098
3 days		2113, 2098

[a] As measured for $[(18\text{-crown-6})K]_3[Cr(CN)_6]$.

Consequently, the IR stretches of complexes **2** and **3** that appear at ~20 cm^{-1} higher than the ν(C≡N) of the free $[M^{III}(CN)_6]^{3-}$ ions are assigned to the bridging CN^- ligands.

For compounds **4** and **5**, the expected characteristic IR bands were observed (Table 6).[14,24,33] It should be noted at this point that the stretch for complex 4 located at 2096 cm^{-1} is significantly lower than the ν(C≡N) mode for the free $[Cr^{III}(CN)_6]^{3-}$ ion (2116 cm^{-1}) or of any possible cyanide-bridged species that could result from the reaction of $[Co^{II}(dppe)_2(H_2O)]^{2+}$ and $[Cr^{III}(CN)_6]^{3-}$; as such, its appearance can be easily monitored by solution IR spectroscopy. The slow formation of **4** from the reaction of $[Co^{II}(dppe)_2(H_2O)]^{2+}$ and $[Cr^{III}(CN)_6]^{3-}$ in acetonitrile prompted us to perform a detailed solution IR study of this reaction in order to obtain insight into the mechanism of the dissociation of $[Cr^{III}(CN)_6]^{3-}$.

The solution IR study was carried out by taking a ~1 mL aliquot from the reaction mixture at various intervals (Table 6 and Figure 4). The first aliquot was collected immediately after mixing the solutions of $[Cr^{III}(CN)_6]^{3-}$ and $[Co^{II}(dppe)_2(H_2O)]^{2+}$. The IR spectrum of this first aliquot contains two ν(C≡N) stretches at 2140 and 2113 cm^{-1}. The latter feature corresponds to the ν(C≡N) stretch observed for $[Cr^{III}(CN)_6]^{3-}$ in acetonitrile (2115 cm^{-1}), and the former, which is ~30 cm^{-1} higher in energy, is attributed to a CN-bridged species. A second aliquot, collected after 30 min from the beginning of the reaction, shows the same two ν(C≡N) stretches as the first (initial) aliquot, but with two shoulders at ~2130 and 2090 cm^{-1}. A third aliquot collected after 1 h shows an IR stretch at 2130 cm^{-1} which can be attributed to a CN-bridged species and, more importantly, a ν(C≡N) stretch at 2098 cm^{-1} which corresponds to the ν(C≡N) stretch of a bona fide sample of $[Co^{II}(dppe)_2(CN)]^+$. After the reaction had proceeded for 3 days, crystals of $[Co^{II}(dppe)_2(CN)][BF_4]$ (**4**) were obtained, and a fourth aliquot was sampled from the mother liquor. An IR spectrum of this aliquot exhibits two ν(C≡N) stretches at 2112 and 2098 cm^{-1}, with no discernible features at higher frequencies. The feature at 2112 cm^{-1} corresponds to the ν(C≡N) stretch of $[Cr^{III}(CN)_6]^{3-}$ in acetonitrile, and the ν(C≡N) stretch at 2098 cm^{-1} is assigned to $[Co^{II}(dppe)_2(CN)]^+$. The presence of a bridging species in solution cannot be completely ruled out due to the breadth of the signals; nevertheless, we can conclude that the dominant species in solution after 3 days are $[Cr^{III}(CN)_6]^{3-}$ and $[Co^{II}(dppe)_2(CN)]^+$.

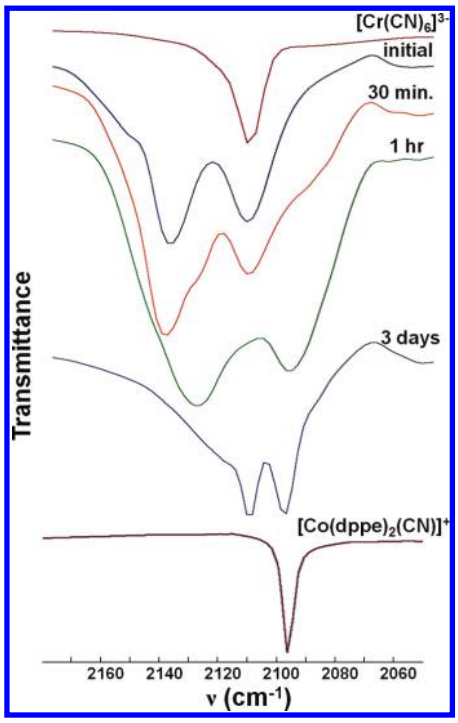

Figure 4. Solution IR spectra from samples taken from the reaction of $[Co^{II}(dppe)_2(H_2O)]^{2+}$ and $[Cr^{III}(CN)_6]^{3-}$ in acetonitrile.

The solution IR data clearly indicate the formation of an initial bridging complex followed by the formation of **4**. The structure of the bridging pentanuclear intermediate **7** that we accidentally isolated suggests that some CN^- ligands of $[Cr^{III}(CN)_6]^{3-}$ are labilized and bind through the carbon ends to the Co^{II} centers. This is a reasonable explanation for the displacement of the chelating dppe ligands observed in the structure of **7**. As monitored by solution IR spectroscopy, the reaction progresses to the stage where there are two dominant ν(C≡N) stretches which correspond to free $[Cr^{III}(CN)_6]^{3-}$ and $[Co^{II}(dppe)_2(CN)]^+$, the latter of which crystallizes from solution as a $[BF_4]^-$ salt. Both solution and solid-state IR data confirm the assignment of the ν(C≡N) stretch to this material.

In addition, solution IR studies of the reaction of $[Co(triphos)(CH_3CN)_2]^{2+}$ and $[M^{III}(CN)_6]^{3-}$ (M = Cr, Fe, and Co) in MeCN were also performed. The IR spectrum of $[Co(triphos)(CH_3CN)_2]^{2+}$ in acetonitrile exhibits two ν(C≡N) stretches at 2317 and 2300 cm^{-1} (Table 7), values that are in reasonable accord with those reported for $[Co^{II}(CH_3CN)_6][BF_4]_2$[34] (2292 and 2316 cm^{-1}). The first aliquot of the $[Co(triphos)(CH_3CN)_2]^{2+}/[Cr^{III}(CN)_6]^{3-}$ (2:1) reaction mixture collected after 5 min contains peaks at 2115, 2300, and 2317 cm^{-1} associated with the reactants, along with three new ν(C≡N) stretches at 2146, 2164, and 2170 cm^{-1} that are in the region of cyanide-bridged species. Aliquots collected after 1 and 3 h exhibit the same features, the only significant difference being a decrease in the intensity of

(33) Rigo, P.; Longato, B.; Favero, G. *Inorg. Chem.* **1972**, *11*, 300–303.

(34) Hathaway, B. J.; Holah, D. G.; Underhill, A. E. *J. Chem. Soc.* **1962**, 2444–2448.

Table 7. Summary of the ν(C≡N) Stretches for Reaction Solutions of $[Co^{II}(triphos)(CN)_2]^{2+}$ with $[M^{III}(CN)_6]^{3-}$ (M = Cr, Fe, Co) in Acetonitrile[a]

$[Co(triphos)(CH_3CN)_2]^{2+}$ + $[M^{III}(CN)_6]^{3-}$	ν(C≡N), cm^{-1}	
	bridging	terminal
$[Co(triphos)(CH_3CN)_2]^{2+}$		2300, 2317
$[Cr^{III}(CN)_6]^{3-}$		2115[b]
initial	2146, 2164, 2170	2300, 2317, 2115
1 h	2146, 2164, 2170	2300, 2317, 2115
2 days		2115, 2101, 2097
$[Co(triphos)(CN)_2]$		2101, 2096
$[Fe^{III}(CN)_6]^{3-}$		2116[b]
initial	2141	2116
1 h	2141, 2152(sh)[c]	2116
2 days	2141, 2152(sh)[c]	2116
$[Co^{III}(CN)_6]^{3-}$		2127[b]
initial	2145, 2165, 2174(sh)	2127
1 h	2145, 2165, 2174(sh)	2127
2 days	2145, 2165, 2174	2127

[a] IR stretches in bold correspond to new species formed in solution. [b] As measured for acetonitrile solutions of $[(18\text{-crown-6})K]_3[Cr(CN)_6]$, $[TMA]_3[Fe(CN)_6]$ and $[(18\text{-crown-6})K]_3[Co(CN)_6]$. [c] sh = shoulder.

the ν(C≡N) stretches of the reactants as compared to those of the product cyanide-bridged species. The last aliquot (collected after two days) exhibits stretches corresponding to the starting materials as well as two new stretches at 2097 and 2101 cm^{-1} and no evidence for the previously observed ν(C≡N) stretches assigned to the CN-bridged species. The new stretches at 2097 and 2101 cm^{-1} are due to the presence of $Co(triphos)(CN)_2$ (**6**).

The solution IR study revealed that the reaction between $[Co(triphos)(CH_3CN)_2]^{2+}$ and $[Cr^{III}(CN)_6]^{3-}$ results in the formation of intermediate cyanide-bridged species. The latter react further to form **6** via labilization of cyanide ligands from $[Cr(CN)_6]^{3-}$, which are sequestered by the low-spin Co^{II} complex. Lability of the cyanide ligand is observed only in the case of $[Cr(CN)_6]^{3-}$. Reactions of $[Co(triphos)(CH_3CN)_2]^{2+}$ with $[Fe(CN)_6]^{3-}$ and $[Co(CN)_6]^{3-}$ result in cyanide-bridged species whose ν(C≡N) stretches are persistent in the IR spectra of the aliquots collected after two days (2141 and 2152 cm^{-1} and 2146, 2164, and 2173 cm^{-1}, respectively). Attempts to crystallize these cyanide-bridged species were unsuccessful.

We also performed an IR study of different forms of the TBP complex **8** obtained under different reaction conditions (Table 1). In a previous study, we investigated a whole family of such complexes formed with different transition metals, and the majority of them exhibit two ν(C≡N) stretches, one that is very close in energy to the free hexacyanometallate anion and the other which is higher in energy by ~20−30 cm^{-1}. These bands are assigned to terminal and bridging CN^- ligands, respectively. All samples of **8** reveal the presence of these two bands (Figure 5).

Note that three of the five samples exhibit a third band at ~2103 cm^{-1}. The latter feature is assigned to the Co−C≡N−Cr configuration of the CN^- bridge. Indeed, this band is the most intense in sample **8a**, which, according to the preparation conditions, should exhibit the highest degree of cyanide linkage isomerism. Moreover, the absorption at 2057 cm^{-1}, assigned to the normal

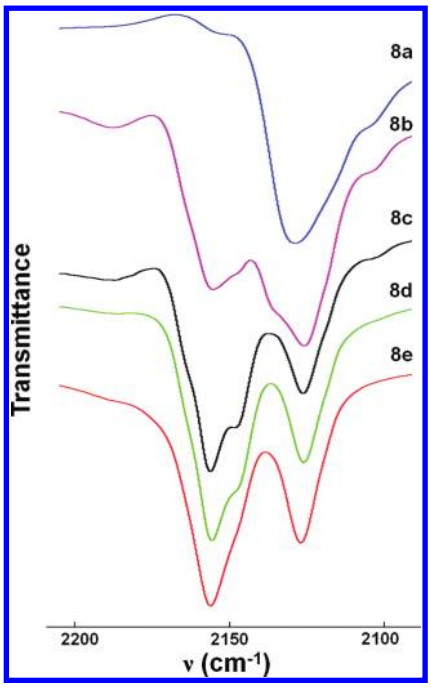

Figure 5. Cyanide stretching bands in the IR spectra of complex **8** prepared by varying the Co(II) starting material, solvent, time, and temperature of the reaction (**8a**: $CoCl_2$ in MeCN, 24 h, 25 °C. **8b**: $Co(BF_4)_2\cdot 6H_2O$ in MeCN, 24 h, 25 °C. **8c**: $Co(BF_4)_2\cdot 6H_2O$ in MeCN, 5 min, 25 °C. **8d**: $Co(BF_4)_2\cdot 6H_2O$ in MeCN, 1 min, 0 °C. **8e**: $CoCl_2\cdot 6H_2O$ in MeOH, 24 h, 25 °C).

Co−N≡C−Cr bridging mode, exhibits very low intensity in this sample. In sample **8b**, the intensity of the higher-frequency band increases at the expense of the lower-frequency band at 2103 cm^{-1}, in accord with the faster crystallization of this sample as compared to **8a** and a lower degree of cyanide reversal. This trend continues for sample **8c**, the rapid precipitation of which was enhanced by stirring the mixture. For samples **8d** and **8e**, the band at 2103 cm^{-1} is absent, a confirmation that a lower reaction temperature or the use of methanol as solvent results in a slower rate of CN^- bridge reversal. The magnetic data, however, reveal that appreciable cyanide linkage isomerism has taken place even in these two samples. It must be pointed out that sample **8e** precipitated instantaneously upon mixing methanolic solutions of the reactants and was kept under the mother liquor for 24 h before being recovered by filtration. Nevertheless, the IR spectrum of this sample is essentially the same as that of sample **8d**, which was isolated from the reaction mixture after stirring for only 1 min at 0 °C. Obviously, the cyanide "flip" occurs rapidly in solution upon formation of the complex. After precipitation of the material, the cyanide bridges remain intact and do not reverse in the solid state.

Magnetic Properties. DC magnetic measurements were performed on freshly prepared crushed polycrystalline samples in the temperature range of 2−300 K in an applied magnetic field of 1000 Oe. Compound **1** exhibits a χT value of 0.68 emu ol^{-1} at 300 K, which is substantially higher than expected for a single $S = 1/2$ center (0.375 emu mol^{-1} K). Upon lowering temperature, the susceptibility decreases linearly to 0.53 emu mol^{-1} K at 2 K (Figure 6a), indicating significant temperature-independent paramagnetism (TIP) of the Van Vleck type, which is due to

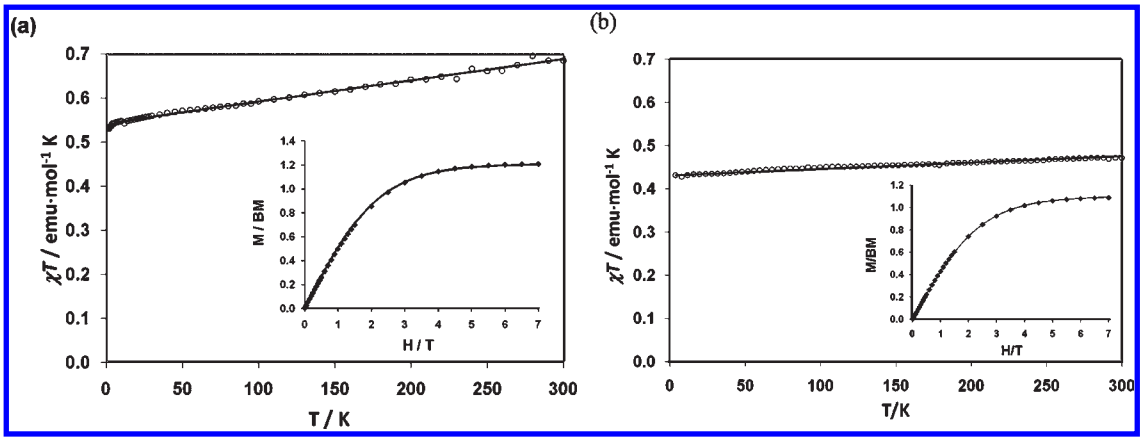

Figure 6. Temperature dependence of χT for (a) compound **1** ($S = 1/2$, $g = 2.41$, TIP $= 4.8 \times 10^{-4}$ emu mol^{-1}, $zJ = -0.1$ cm^{-1}) and (b) compound **4** ($S = 1/2$, $g = 2.20$, TIP $= 1.5 \times 10^{-4}$ emu mol^{-1}). Inset: Field-dependent magnetization curve at 1.8 K. Experimental points are depicted with open circles, and solid lines correspond to the best-fit curves.

low-lying excited states. Both the temperature dependence of χT and the field-dependent magnetization data were satisfactorily fitted to an $S = 1/2$ system with $g = 2.41$ and TIP $= 4.8 \times 10^{-4}$ emu mol^{-1} (Figure 6a). In order to account for the slight decrease of χT at low temperatures, a molecular field correction ($zJ = -0.10$ cm^{-1}) was added to include intermolecular interactions.[35] The 300 K χT value of **4** is slightly lower, namely 0.47 emu mol^{-1} K and decreases linearly to reach 0.43 emu mol^{-1} K at 2 K (Figure 6b). Thus, the TIP contribution is lower (1.5×10^{-4} emu mol^{-1}) compared to that of complex **1**. Such behavior is in agreement with a greater separation between the ground and excited states for **4**, as expected for the stronger ligand field created by the presence of the carbon-bound cyanide in this complex. The temperature dependence of χT and field-dependent magnetization data fit the behavior of an $S = 1/2$ system with $g = 2.20$ (Figure 6b, inset).

Compound **2** exhibits a value of $\chi T = 0.95$ emu mol^{-1} K at 300 K, higher than the spin-only value expected for two noninteracting low-spin $S = 1/2$ Co^{II} ions (0.75 emu mol^{-1} K). The susceptibility value decreases linearly as the temperature is lowered (Figure 7), once again due to the TIP contribution of Co^{II} ions (2.1×10^{-4} emu mol^{-1} per ion). The sharp decrease in the susceptibility at very low temperatures is due to intramolecular antiferromagnetic exchange between $S = 1/2$ Co^{II} centers through the diamagnetic Co^{III} ion ($J = -0.4$ cm^{-1}). The same model satisfactorily describes the field-dependent magnetization data (Figure 7, inset).

For compound **3**, the χT value at 300 K is 1.72 emu mol^{-1} K, which is higher than the spin-only value of 1.13 emu mol^{-1} K expected for two noninteracting low-spin $S = 1/2$ Co^{II} ions and one low-spin $S = 1/2$ Fe^{III} ion. Such a deviation is mainly due to the significant orbital contribution characteristic of the orbitally degenerate $^2T_2$ ground state of the low-spin Fe^{III} ion and the TIP contribution of Co^{II} ions, as observed in the isostructural complex **2**. The value of χT decreases upon cooling until $T \sim 60$ K, and then abruptly increases to a maximum of 1.87 emu mol^{-1} K at ~ 6 K (Figure 8), which is indicative of the stabilization of an $S = 3/2$ ground state,

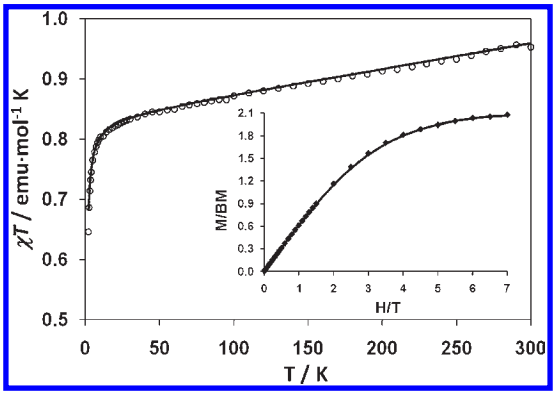

Figure 7. Temperature dependence of χT for **2** (two $S = 1/2$ centers, $g = 2.11$, TIP $= 2.1 \times 10^{-4}$ emu mol^{-1}, $J = -0.4$ cm^{-1}). Inset: Field-dependent magnetization curve at 1.8 K. Experimental points are shown with open circles. Solid lines correspond to theoretical simulations obtained with MAGPACK.[36]

suggesting a ferromagnetic superexchange between the Co^{II} and Fe^{III} centers rather than antiferromagnetic coupling, which would result in an $S = 1/2$ ground state. It must be noted that the gradual decrease of χT from room temperature cannot be taken as an indication of antiferromagnetic coupling because spin−orbit coupling of the low-spin Fe^{III} ion and the TIP of the Co^{II} centers are important contributors. For comparison, Figure 8 depicts the sum of χT plots for compound **2** and $(TBA)_3[Fe(CN)_6]$. The χT versus T dependence for **3** shows an obvious deviation to higher values as compared to the combined curve. This deviation increases with decreasing temperature, thus confirming that remote ferromagnetic coupling is occurring between the Co^{II} and Fe^{III} centers in **3**. Stabilization of the high-spin ground state was further corroborated by field-dependent magnetization data (Figure 8, inset), which saturate at a value of 3.05 μ_B as expected for a ferromagnetic $S = 3/2$ ground state. The observed decrease in χT below 6 K and the slight deviation of the magnetization data from the Brillouin function calculated for $S = 3/2$ are attributed to the weak intermolecular antiferromagnetic interactions and zero-field splitting effects.

Due to the varying degrees of cyanide linkage isomerism observed in samples of compound **8** (Table 1), an accurate

(35) Carlin, R. L. *Magnetochemistry* **1986**, 328.

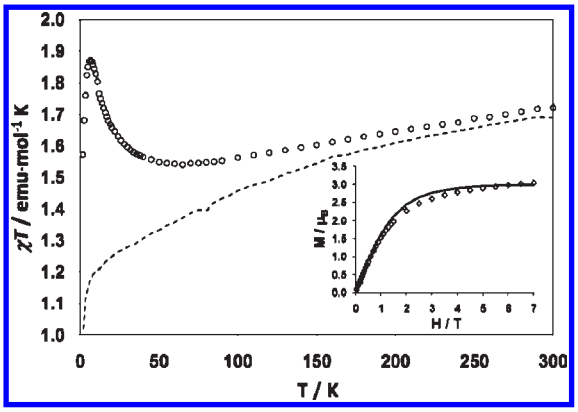

Figure 8. Temperature dependence of χT for **3**. For comparison, the dashed line shows a combined contribution from isostructural complex **2** and $TBA_3[Fe(CN)_6]$ (see the text). Inset: Field-dependent magnetization at 1.8 K, with the solid line depicting the Brillouin function for $S = 3/2$, $g = 2.00$.

treatment of its magnetic behavior is not possible. Nevertheless, the magnetic properties of the samples follow the qualitative trend expected for the mixture of isomerized and nonisomerized TBP clusters. First of all, we note that, in the nonisomerized form, each Co^{II} ion is equipped with two tmphen ligands and two N-bound cyanides. As demonstrated previously by our study of the model compound $\{[Co^{II}(tmphen)_2]_3[Co^{III}(CN)_6]_2\}$, such a coordination results in a high-spin $S = 3/2$ state for the Co^{II} centers.[21] After the cyanide flipping event, however, the equatorial Co^{II} ions are coordinated to the strong-field C-bound end of the CN^- ligands and are in the low-spin $S = 1/2$ state.[37] (Of course, intermediate forms of the cluster can exist, in which cyanide bridges are only partially reversed, but the overall trend for the Co^{II} centers to assume the low-spin electronic configuration upon increasing the extent of cyanide linkage isomerism is evident.)

The conversion of the equatorial Co^{II} ions from the high-spin $S = 3/2$ to the low-spin $S = 1/2$ state results in a spin-pairing of electrons in the t_{2g} orbitals and has two major ramifications on the magnetic behavior of **8**: (1) The room-temperature value of χT decreases as the degree of cyanide flip increases. As a means of comparison, the dashed line in Figure 9 shows a combined contribution from three equatorial high-spin $S = 3/2$ Co^{II} and two axial $S = 3/2$ Cr^{III} ions in the absence of magnetic coupling. This was calculated by adding the χT versus T dependences of the model compounds $\{[Co^{II}(tmphen)_2]_3[Co^{III}(CN)_6]_2\}$ and $\{[Zn^{II}(tmphen)_2]_3[Cr^{III}(CN)_6]_2\}$,[21] which contain diamagnetic metal ions in the axial and equatorial positions, respectively. (2) The ferromagnetic coupling between the Co^{II} and Cr^{III} centers becomes stronger as the cyanide linkage isomerism occurs. This fact has been explained by the removal of the antiferromagnetic contribution to the $Co^{II}-Cr^{III}$ magnetic superexchange upon going from the high-spin $t_{2g}^5e_g^2$ to the low-spin $t_{2g}^6e_g^1$ Co^{II} ion.[21] Indeed, the high-temperature part of the χT versus T curve is much steeper for sample **8a**

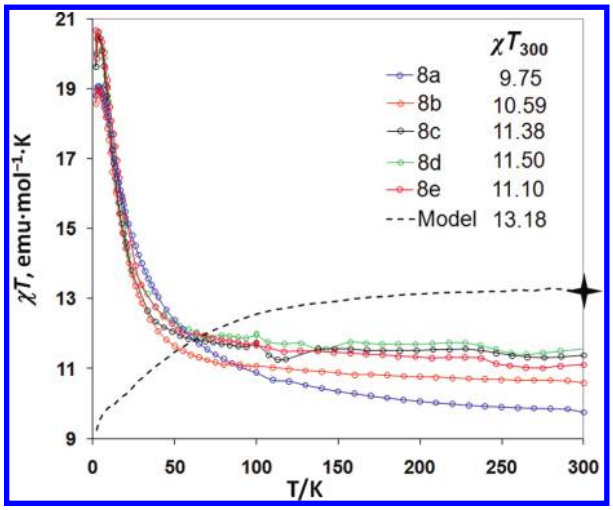

Figure 9. Temperature dependence of χT for different samples of **8**. The solid lines are guides for the eye. The dashed line represents a combined contribution from two model isostructural complexes, namely, $\{[M(tmphen)_2]_3[M'(CN)_6]_2\}$ (M = Co/Co and Zn/Cr; see the text).

(Figure 9), for which the extent of cyanide flip is the greatest; this observation is in accord with stronger ferromagnetic exchange.

Conclusions

Contrary to the commonly held notion that Cr^{III} is a rather inert ion due to the half-filling of its t_{2g} orbitals, we found that the presence of certain Lewis acids (e.g., Co^{II} and Fe^{II} ions, BPh_3) leads to facile labilization of cyanide ligands from the $[Cr(CN)_6]^{3-}$ anion. Results of the detailed study presented herein obtained by a combination of X-ray crystallography, infrared spectroscopy, and magnetic measurements provide unequivocal evidence for this phenomenon during reactions of various Co^{II} complexes with the hexacyanochromate(III) anion. The final products of such reactions are mono- or polynuclear complexes in which the CN^- ligand is carbon-bound to the Co^{II} ion rather than to the Cr^{III} center. Reactions of $[Co(dppe)_2(H_2O)](BF_4)_2$ and $[Co(triphos)(CH_3CN)_2](BF_4)_2$ with $[Cr(CN)_6]^{3-}$ yield the mononuclear complexes $[Co(dppe)_2(CN)](BF_4)$ and $[Co(triphos)(CN)_2]$, respectively. In the former case, we were able to isolate the pentanuclear intermediate $\{[Co^{II}{}_3(dppe)_4(MeCN)][Cr^{III}(CN)_6]_2\}$. A study of this reaction by solution IR spectroscopy reveals a gradual conversion of the $\nu(C\equiv N)$ stretches of the starting materials to those of the CN-bridged intermediate and finally to the single $\nu(C\equiv N)$ stretch of the mononuclear product. The loss of carbon-bound CN^- ligands from $[Cr(CN)_6]^{3-}$ is on a sufficiently slow time-scale for observation of varying degrees of cyanide linkage isomerism in the trigonal-bipyramidal complex $\{[Co(tmphen)_2]_3[Cr(CN)_6]_2\}$, aided by the use of different Co^{II} starting materials. The varying extent of the cyanide flip in this complex leads to a variable ratio of the N-coordinated high-spin $S = 3/2$ form to the C-coordinated low-spin $S = 1/2$ Co^{II} form, a fact that is reflected in the magnetic behavior of the mixtures. These results are in contrast to the fast and complete reversal of cyanide bridges that we observed in the chemistry

(36) Borras-Almenar, J. J.; Clemente-Juan, J. M.; Coronado, E.; Tsukerblat, B. S. *J. Comput. Chem.* **2001**, *22*, 985–991.
(37) Jian, F. F.; Xiao, H. L.; Li, L.; Sun, P. P. *J. Coord. Chem.* **2004**, *57*, 1131–1137.

leading to $\{[Fe(tmphen)_2]_3[Cr(CN)_6]_2\}$ and $(Et_4N)_3[Cr(NCBPh_3)]$.

Acknowledgment. The authors would like to thank Dr. Joseph H. Reibenspies for his help with single-crystal X-ray crystallography. This research was supported by the NSF (PI grant CHE-0610019) and partially by the DOE (grant DE-FG03-02ER45999). K.R.D. gratefully acknowledged financial support from the Welch Foundation (A-1449). Funding of the CCD diffractometer (CHE-9807975) and the SQUID magnetometer (NSF 9974899) by the NSF is also gratefully acknowledged.

Supporting Information Available: Crystallographic files in CIF format. This material is available free of charge via the Internet at http://pubs.acs.org.